imately 8 h of reaction time, leads to the loss of catalytic activity for peroxide decomposition.

Acknowledgment. We thank Dr. S. Davis of the Monsanto Co. for the analysis of the high-boiling products in the oxidation reactions, as well as Dr. D. Druliner of Du Pont for running the reaction under industrial conditions. We also acknowledge the Army Research Office and the National Science Foundation for their financial support.

Registry No. $[Co(NCCH_3)_4](PF_6)_2$, 136794-37-1; cyclohexane, 110-82-7; adamantane, 281-23-2; cyclohexanol, 108-93-0; cyclohexanone, 108-94-1; 1-adamantanol, 768-95-6; 2-adamantanol, 700-57-2; 2-adamantanone, 700-58-3.

Contribution from the Department of Chemistry, University of Florence, 50121 Florence, Italy, and Department of Biochemistry, University of British Columbia, Vancouver, British Columbia V6T 1Z3 Canada

Comparative ^1H NMR Study of Ferric Low-Spin Cytochrome *c* Peroxidase and Horseradish Peroxidase

Lucia Banci,[†] Ivano Bertini,*[,†] Paola Turano,[†] Juan C. Ferrer,[‡] and A. Grant Mauk[‡]

Received February 28, 1991

Proton NMR spectra of the cyanide complexes of cytochrome *c* peroxidase from baker's yeast (CcP) and recombinant protein expressed in *Escherichia coli* (MKT-IGCcP) have been recorded in water. The paramagnetically shifted exchangeable proton signals have been assigned through NOE and NOESY experiments. NOESY and COSY experiments in D_2O and H_2O buffers have allowed us to extend the assignments to heme substituents and other residues. Comparison is made with the analogous spectrum of the cyanide adduct of horseradish peroxidase (HRP) (Thanabal, V.; de Ropp, J. S.; La Mar, G. N. *J. Am. Chem. Soc.* **1988**, *110*, 3027). HRP-CN^- and CcP-CN^- systems are highly analogous as shown by the similarity of the pseudocontact shifts of the distal histidine protons and by the protonation status of the proximal and distal histidine in both systems. A more extensive exchangeable proton connectivity network is observed in CcP-CN^-. Small but significant structural differences have been identified in the orientation of the proximal histidyl residues of HRP-CN^- and CcP-CN^- and in the interresidue distances in the distal heme pocket of CcP-CN^- and MKT-IGCcP-CN^- as a function of the identity of the residue present at position 53.

Peroxidases are a class of heme proteins that react with H_2O_2 or alkyl peroxides to perform a variety of oxidation reactions.[1] Among peroxidases, cytochrome *c* peroxidase (CcP) and horseradish peroxidase (HRP) have been studied in greatest detail by a variety of physical and spectroscopic techniques.[1] In the resting state, the heme iron of most peroxidases is high-spin Fe(III), though the HRP heme iron has been proposed to possess a spin admixture with $S = {}^3/_2$.[2] The fifth coordination position of the Fe(III) ion in peroxidases is occupied by the nitrogen atom of a histidyl residue (the proximal histidine)[3] in all known members of this family. Characterization of the sixth coordination position of peroxidases in the resting state has been the subject of intense study.[3d,4]

While HRP in the resting state is thought to be five-coordinate,[4c] a consensus concerning the coordination environment of resting state CcP has been more difficult to achieve.[4] Refined structural models have been reported for the ferric ("resting state") enzyme[3b] and for the CN^- adduct.[5] The two structures are highly similar except for the movement of the iron atom toward the heme plane and the removal of one water molecule from the distal side of the heme upon CN^- binding. Several critical amino acid residues and water molecules occurring on both sides of the heme prosthetic group in the CN^--bound form of the protein are illustrated in Figure 1.

Reaction of peroxidases with H_2O_2 produces the active oxidizing form of the protein, the electronic structure of which varies between peroxidases. Historically, this form of CcP is referred to as compound ES, and the corresponding form of HRP is referred to as compound I.[1] Despite the close similarity in heme iron coordination geometries of HRP compound I and CcP compound ES,[6] their electronic structures are substantially different. Both derivatives are oxidized by 2 equiv above the resting enzyme and possess a ferryl heme iron (Fe^{IV}=O); however, they differ in that compound ES possesses a radical centered on Trp-191[7] while HRP possesses a porphyrin π-cation-radical center.[8]

Both resting enzymes bind cyanide as a sixth ligand to produce a species with low-spin Fe(III); the three-dimensional structure of CcP-CN^- has been reported recently (Figure 1).[5] Binding of cyanide displaces the water molecule that is located closest to the iron atom and results in a rearrangement of the hydrogen-bonding pattern of the remaining two water molecules;[5] both of the remaining water molecules form hydrogen bonds with the nitrogen atom of the cyanide group. One of these water molecules also forms a hydrogen bond with Arg-48. Crystallographic analysis also reveals that Arg-48, Trp-51, and His-52 are all within hydrogen-bonding distance of the cyanide nitrogen atom. As hydrogen bond formation with the bound cyanide anion requires hydrogen atom donation by the putative hydrogen bonding partner, Arg-48 and Trp-51 are both capable of hydrogen bonding to this group as both groups meet this requirement. However, it is not currently apparent whether or not His-52 meets this criterion because the protonation status of this residue cannot be determined from the current structural model of the protein.[5]

Assignments of the ^1H NMR spectrum of HRP-CN^- has been one of the most elegant applications of ^1H NMR spectroscopy

[†] University of Florence.
[‡] University of British Columbia.

(1) (a) Caughey, W. S. *Inorganic Biochemistry*; Eichorn, G. L., Ed.; Elsevier: Amsterdam, 1973; Vol. 2, Chapter 24. (b) Dunford, H. B.; Stillman, J. S. *Coord. Chem. Rev.* **1976**, *19*, 187. (c) Morrison, M.; Schonbaum, G. R. *Annu. Rev. Biochem.* **1979**, *45*, 861. (d) Dunford, H. B. *Adv. Inorg. Chem.* **1982**, *4*, 41. (e) Poulos, T. L. *Adv. Inorg. Biochem.* **1988**, *7*, 1. (f) *Peroxidases in Chemistry and Biology*; Everse, J., Everse, K. E., Grisham, M. B., Eds.; CRC Press: Boca Raton, 1990; Vols. 1 and 2.
(2) La Mar, G. N.; de Ropp, J. S.; Smith, K. M.; Langry, K. C. *J. Biol. Chem.* **1980**, *255*, 6646.
(3) (a) Poulos, T. L.; Kraut, J. *J. Biol. Chem.* **1980**, *255*, 8199. (b) Finzel, B. C.; Poulos, T. L.; Kraut, J. *J. Biol. Chem.* **1984**, *259*, 13027. (c) Sakurda, J.; Takahashi, S.; Hosoya, T. *J. Biol. Chem.* **1986**, *261*, 9657. (d) Dawson, J. H. *Science* **1988**, *240*, 433.
(4) (a) Evangelista-Kirkup, R.; Cristanti, M.; Poulos, T. L.; Spiro, T. G. *FEBS Lett.* **1985**, *190*, 221. (b) Yonetani, T.; Anni, H. *J. Biol. Chem.* **1987**, *262*, 9547. (c) La Mar, G. N.; Chatfield, M. J.; Peyton, D. H.; de Ropp, J. S.; Smith, W. S.; Krishnamoorthi, R.; Satterlee, J. D.; Erman, J. E. *Biochim. Biophys. Acta* **1988**, *956*, 267.
(5) Edwards, S. L.; Poulos, T. L. *J. Biol. Chem.* **1990**, *265*, 2588.
(6) Chance, M.; Powers, L.; Poulos, T.; Chance, B. *Biochemistry* **1986**, *25*, 1266.
(7) (a) Sivraja, M.; Goodin, D. B.; Smith, M.; Hoffman, B. M. *Science* **1989**, *245*, 738. (b) Erman, J. E.; Vitello, L. B.; Mauro, J. M.; Kraut, J. *Biochemistry* **1989**, *28*, 7992.
(8) Dolphin, D.; Forman, A.; Borg, D. C.; Fajer, J.; Felton, R. H. *Proc. Natl. Acad. Sci. U.S.A.* **1971**, *68*, 614.

0020-1669/91/1330-4510$02.50/0

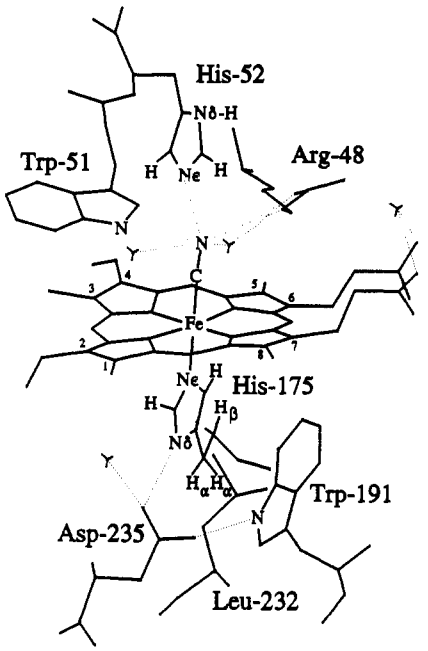

Figure 1. Active site of the cyanide complex of yeast cytochrome *c* peroxidase.[5] The residues and hydrogen atoms discussed in the text and in Table I are indicated.

to paramagnetic systems. The heme methyl protons have been assigned through their selective deuteration[9] while the other heme proton signals have been assigned through NOE[10] and saturation transfer experiments.[10b] The signals of the proximal imidazole are also assigned,[10] and the shift of Hε1 is taken as evidence of the extent of imidazolate character.[10c] Finally, the distal histidine protons have been assigned, and it has been shown that anion binding favors stabilization of the imidazolium ion.[10c]

Related NMR studies have also been reported for CcP.[11] As for HRP, many heme resonances have been assigned through deuteration,[11b,c] and the nonexchangeable signals of the proximal histidine, heme vinyl, and heme propionate side chains have been assigned through NOE experiments.[11e] However, when this paper was submitted, no published NMR studies of CcP–CN^- had been performed in water, so the resonances attributable to the exchangeable protons had not been assigned. In the course of initial studies involving mutant forms of CcP, we have reanalyzed the ^1H NMR spectra of both HRP–CN^- and CcP–CN^- to assign the exchangeable histidyl protons in the active site of CcP, to compare the spectra of the two proteins, and to correlate the properties of the two proteins with the electronic structure of the heme Fe(III) ion. Well after this manuscript was submitted, a paper appeared[12] that describes the ^1H NMR spectrum of CcP–CN^-, also in water, and that only partially agrees with the present data.

Materials and Methods

Horseradish peroxidase (Sigma, Type VI) was obtained as a lyophilized, salt-free powder and used without further purification. Cytochrome *c* peroxidase from baker's yeast (Red Star, Milwaukee, WI) was provided by Professor Brian Hoffman's laboratory; we refer to this form of the enzyme as CcP. Recombinant yeast cytochrome *c* peroxidase was expressed in *Escherichia coli*[13] and purified by slight modification of a published procedure.[14] As described elsewhere,[13] the three amino terminal residues of this recombinant enzyme have been changed to Met-Lys-Thr to improve protein expression. Furthermore, the CcP gene isolated by Blobel and co-workers[15] and used in this work codes for a protein that differs in sequence from the enzyme isolated from commercial yeast in that Thr-53 is an Ile residue and Asp-152 is a Gly residue. We refer to this recombinant enzyme, therefore, as MKT-IGCcP. The ^1H NMR samples were prepared by dissolving or exchanging the proteins into phosphate buffer (0.05–0.1 M), adding excess solid KCN, and adjusting the pH to 6.3.

The ^1H NMR spectra were recorded with a Bruker 200 MSL spectrometer. T_1 measurements were performed by using the inversion recovery pulse sequence.[16] The NOE measurements were performed by using a superWEFT[17] pulse sequence with a recycle delay of 220 ms. Difference spectra were collected as described previously.[18] NOE experiments on exchangeable protons (b and e) were also collected by using the 1331 pulse sequence as the observing pulse,[19] thus avoiding the excitation of the water resonance.

A number of NOE measurements on paramagnetic systems are available in the literature.[10,18,20] Steady-state NOEs among the fast relaxing signals allowed us to neglect spin diffusion. The steady-state NOE η_i on proton H_i upon saturation of resonance H_j is given by

$$\eta_i = \sigma_{ij} T_{1\text{isel}}$$

where σ_{ij} is the cross-relaxation rate between H_i and H_j, and $T_{1\text{isel}}$ is the selective spin–lattice relaxation time of H_i, which, in the present case, has been taken equal to the nonselective T_1. This is a good approximation in paramagnetic systems, where the nuclear relaxation rates are dominated by the coupling with the unpaired electrons. In turn, σ_{ij} is proportional to the inverse of the sixth power of the interproton distance.

2D NOESY and COSY spectra were recorded at 600 MHz by using presaturation to eliminate the water signal. The NOESY experiment[21]

Table I. Chemical Shift and T_1 Values Observed for Paramagnetically Shifted Resonances for the Cyanide Derivatives of CcP, MKT-IGCcP, and HRP (Phosphate Buffer, 0.05 M; pH 6.3; 301 K) for Resonances Outside the Diamagnetic Envelope

	CcP–CN^-		MKT-IGCcP–CN^-		HRP–CN^-		
signal	shift, ppm	T_1, ms	shift, ppm	T_1, ms	shift, ppm	T_1, ms	assign[a]
A	30.6	40	30.6	39	26.0	57	3-CH_3
a	28.4	7	29.0	*b*	31.0	*b*	Hε2 His-52
B	27.6	39	28.1	40	31.0	44	8-CH_3
C	19.4	34	19.6	29	23.7	21	Hβ His-175
D	18.3	45	18.5	43	19.6	83	7-Hα
b	17.8	13	17.3	14	*c*	*c*	Arg-48
c	16.5	*b*	16.8[d]	*b*	16.3	260	Hδ1 His-52
E	16.0	60	16.5	*b*	20.1	96	4-Hα
H′	15.8	*b*	17.6	*b*	20.8	*b*	Hδ2 His-175
F	14.8	34	14.9	35	15.6	41	Hβ His-175
G	14.0	67	13.9	69	13.3	42	Hε1 His-52
d	12.9	110	13.0	140	12.9	238	NH_p His-175
e′	12.3	200	12.2	200	12.9	239	Arg-48
f	10.2[d]	*b*	10.1[d]	*b*	9.9[d]	*b*	Hδ1 His-175
Y	−2.6	*b*	−2.8	*b*	−3.2	*b*	δ-CH_3 Leu-232
Z	−20.6	2.5	−22.2	2.6	−29.9	2.7	Hε1 His-175

[a] Numbering of amino acids is referred to the CcP sequence. [b] Not measured because the signal is in a complex envelope. [c] The corresponding signal is not present in HRP. [d] The shift value is measured in NOE difference spectra.

(9) de Ropp, J. S.; La Mar, G. N.; Smith, K. M.; Langry, K. C. *J. Am. Chem. Soc.* **1984**, *106*, 4438.
(10) (a) Thanabal, V.; de Ropp, J. S.; La Mar, G. N. *J. Am. Chem. Soc.* **1986**, *108*, 4244. (b) Thanabal, V.; de Ropp, J. S.; La Mar, G. N. *J. Am. Chem. Soc.* **1987**, *109*, 265. (c) Thanabal, V.; de Ropp, J. S.; La Mar, G. N. *J. Am. Chem. Soc.* **1987**, *109*, 7516. (d) Thanabal, V.; de Ropp, J. S.; La Mar, G. N. *J. Am. Chem. Soc.* **1988**, *110*, 3027.
(11) (a) La Mar, G. N.; de Ropp, J. S.; Chacko, V. P.; Satterlee, J. D.; Erman, J. E. *Biochim. Biophys. Acta* **1982**, *708*, 317. (b) Satterlee, J. D.; Erman, J. E.; La Mar, G. N.; Smith, K. M.; Langry, K. C. *Biochim. Biophys. Acta* **1983**, *743*, 246. (c) Satterlee, J. D.; Erman, J. E.; La Mar, G. N.; Smith, K. M.; Langry, K. C. *J. Am. Chem. Soc.* **1983**, *105*, 2099. (d) Satterlee, J. D.; Erman, J. E. *Biochim. Biophys. Acta* **1983**, *743*, 149. (e) Satterlee, J. D.; Erman, J. E.; de Ropp, J. S. *J. Biol. Chem.* **1987**, *262*, 11578. (f) Satterlee, J. D.; Erman, J. E.; Mauro, J. M.; Kraut, J. *Biochemistry* **1990**, *29*, 8797.
(12) Satterlee, J. D.; Erman, J. E. *Biochemistry* **1991**, *30*, 4398.
(13) Goodin, D. B.; Davidson, M. G.; Roe, J. A. Manuscript in preparation.
(14) Fishel, L. A.; Villafranca, J. E.; Mauro, J. M.; Kraut, J. *Biochemistry* **1987**, *26*, 351.
(15) Kaput, J.; Goltz, S.; Blobel, G. *J. Biol. Chem.* **1982**, *257*, 15054.
(16) Vold, R. L.; Waugh, J. S.; Klein, M. P.; Phelps, D. E. *J. Chem. Phys.* **1968**, *48*, 3831.
(17) Inubushi, T.; Becker, E. D. *J. Magn. Reson.* **1983**, *51*, 128.
(18) Banci, L.; Bertini, I.; Luchinat, C.; Piccioli, M.; Scozzafava, A.; Turano, P. *Inorg. Chem.* **1989**, *28*, 4650.
(19) Hore, P. J. *J. Magn. Reson.* **1983**, *55*, 283.
(20) Bertini, I.; Luchinat, C. *NMR of Paramagnetic Molecules in Biological Systems*; Benjamin/Cummings: Menlo Park, CA, 1986, and references therein.
(21) Macura, S.; Wüthrich, K.; Ernst, R. R. *J. Magn. Reson.* **1982**, *47*, 351.

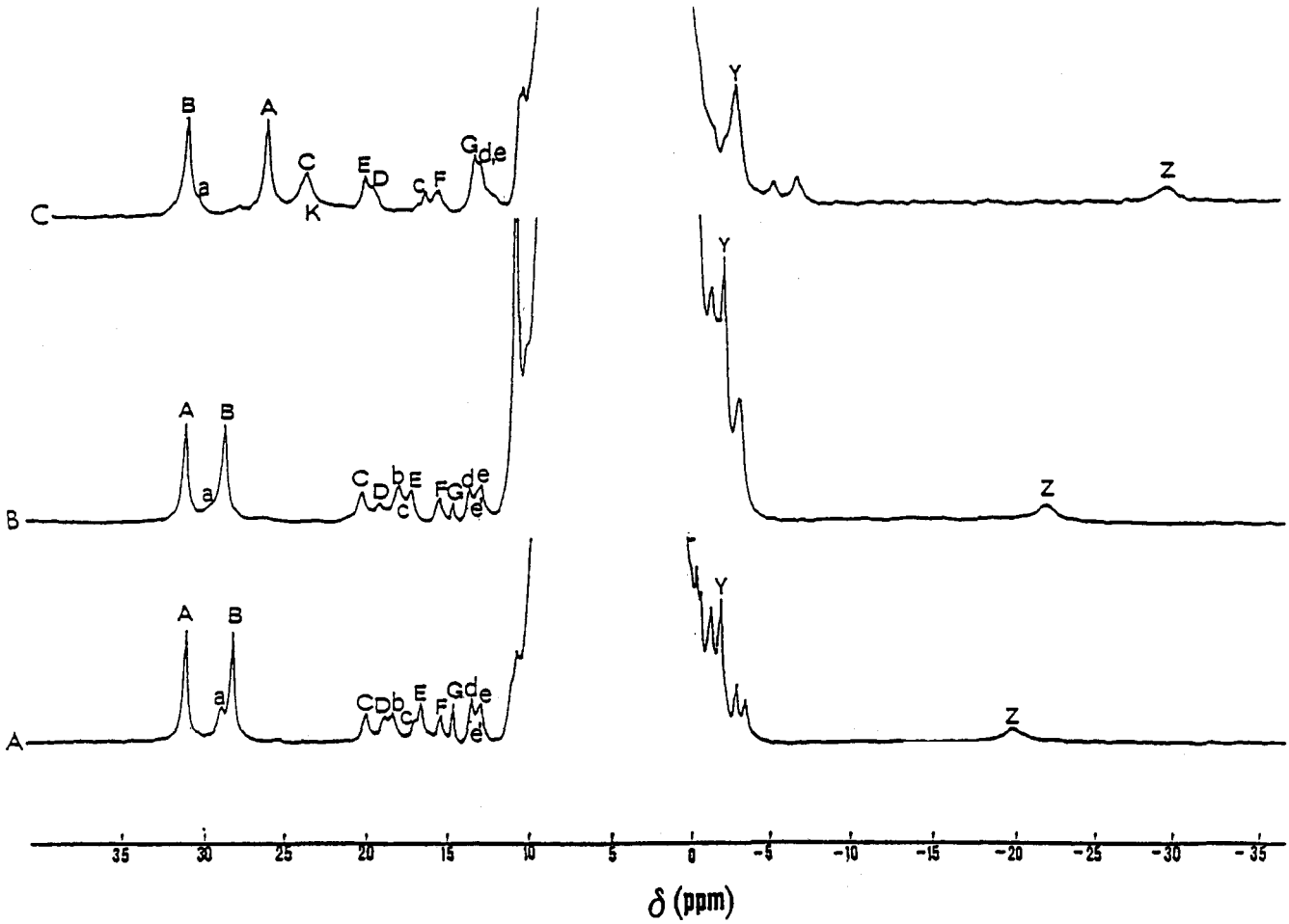

Figure 2. 200-MHz ^{1}H NMR spectra of water solutions (phosphate buffer, pH 6.3, 301 K): (A) C*c*P–CN$^-$; (B) MKT-IGC*c*P–CN$^-$; (C) HRP–CN$^-$.

is the 2D equivalent of the NOE experiment. Phase-sensitive (TPPI)[22] NOESY spectra were recorded at a mixing time of 15 ms to avoid spin diffusion. A total of 512 experiments were collected with a data point number in the F2 direction of 1K. The data were multiplied in both dimensions by a sine-squared bell window function with phase shift of 45° and were zero-filled to obtain 1K × 1K real data points.

Cross peaks in COSY maps detect scalar connectivities. Magnitude COSY[23] experiments provide one of the best sequences for the detection of scalar connectivities in paramagnetic systems.[24,25] In the present case, the best results were obtained by recording magnitude COSY experiments consisting of 512 experiments, with a data point number in the F2 direction of 1K. The data were processed in both dimensions by a pure sine-squared bell window function and zero-filled to obtain 1K × 1K or 2K × 1K real data points.

Results and Discussion

The ^{1}H NMR spectra of HRP–CN$^-$, MKT-IGC*c*P–CN$^-$, and C*c*P–CN$^-$ are shown in Figure 2. The resonances seen in these spectra are labeled similarly for comparison, with lower case letters used to designate exchangeable protons. The chemical shifts, T_1 values, and assignments for the protons of the proximal and distal histidines are set out in Table I. In Table II, the assignments of some protons of heme substituents and of Leu-232 are reported as they result from NOESY and COSY experiments on MKT-IGC*c*P–CN$^-$. The spectra of MKT-IGC*c*P–CN$^-$ and C*c*P–CN$^-$ are quite similar apart from minor shift differences of some exchangeable protons and the chemical shift of signal Z. The exchangeable proton a shows a sharper signal in C*c*P–CN$^-$ when freshly dissolved than does the corresponding resonance in MKT-IGC*c*P–CN$^-$. The line width of this resonance, however, increases a few days after the sample preparation, and the spectra of the two forms of the enzyme, as far as this signal is concerned, become very similar.

Table II. Chemical Shift Values and Assignment of Signals in the "Quasi" Diamagnetic Region of MKT-IGC*c*P–CN$^-$, Obtained through NOESY and COSY Experiments

shift (298 K), ppm	assignt	shift (298 K), ppm	assignt
7.1	2-Hα	−1.3	7-Hβ
6.4	7-Hα'	−2.1	4-Hβ_{trans}
3.0	7-Hβ'	−3.0	2-Hβ_{trans}
0.7	Hγ Leu-232	−3.7	2-Hβ_{cis}
−1.1	δ'-CH$_3$ Leu-232	−3.8	4-Hβ_{cis}

The assignments of the histidyl NH protons were obtained by NOE experiments for the proximal (Figure 3) and distal (Figure 4) histidine residues of C*c*P–CN$^-$ and MKT-IGC*c*P–CN$^-$ and were compared with the NOEs on HRP–CN$^-$. The difference in NOEs between the two proteins is within experimental error. Confirmation of the assignments is obtained by NOESY experiments (Figure 5, cross peaks 28–30). Signal Z (at −29.9 ppm for HRP–CN$^-$, −20.6 ppm for C*c*P–CN$^-$, and −22.2 ppm for MKT-IGC*c*P–CN$^-$) has been assigned to Hϵ1 of the proximal histidine residue.[11a] Saturation of this resonance in HRP–CN$^-$ yields an NOE to the three proton signal at −3.2 ppm and to an exchangeable proton signal at 9.9 ppm that was assigned as Hδ1 of the proximal histidine.[10d] The line width of this exchangeable resonance indicates that this proton is farther from the iron than would be the case if it were associated with a neutral imidazole group. Thanabal et al. attribute this finding to partial imidazolate character of the proximal His that is induced by a putative hydrogen-bonding interaction of this residue with an adjacent Asp residue.[10d]

(22) Marion, D.; Wüthrich, K. *Biochem. Biophys. Res. Commun.* **1983**, *113*, 967.
(23) Aue, W. P.; Bartholdi, E.; Ernst, R. R. *J. Chem. Phys.* **1976**, *64*, 2229.
(24) Yu, L. P.; La Mar, G. N.; Rajanathnam, K. *J. Am. Chem. Soc.* **1990**, *112*, 9527.
(25) Bertini, I.; Capozzi, F.; Luchinat, C.; Turano, P. *J. Magn. Reson.*, in press.

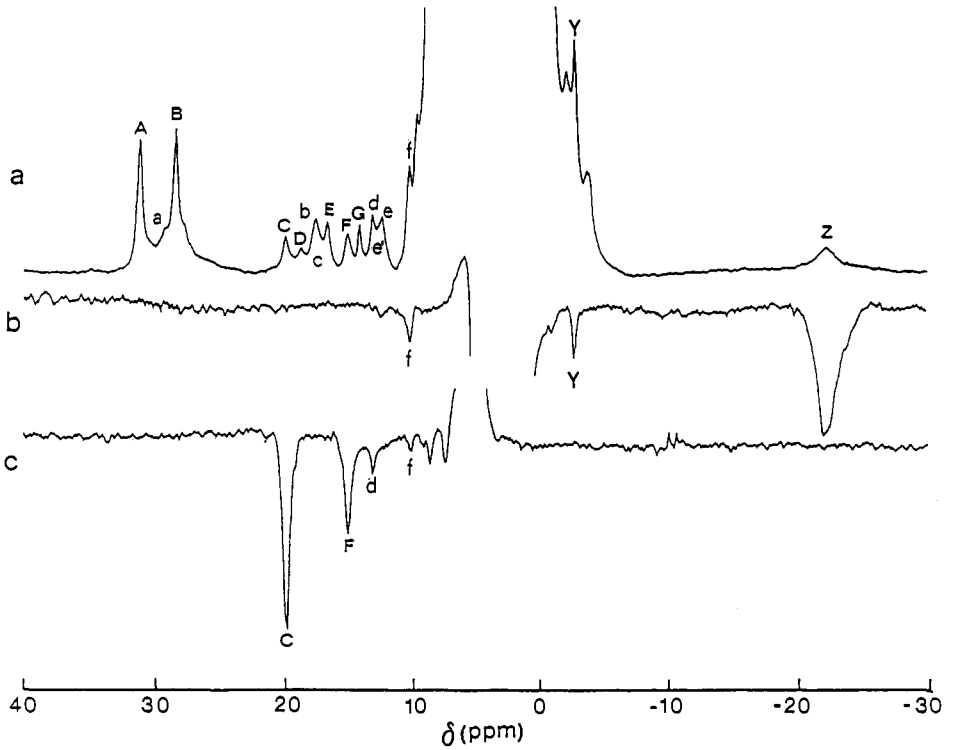

Figure 3. 200-MHz ^{1}H NMR spectrum of a water solution of MKT-IGC*c*P–CN$^-$. Traces b and c are the NOE difference spectra obtained upon saturation of signal Z and C, respectively. The conditions are as in Figure 2, except for the temperature, which is 296 K.

The chemical shift for the Hδ1 proton of the proximal histidine in C*c*P–CN$^-$ has not been identified previously. Saturation of the upfield signal assigned to Hϵ1 of His-175 (the proximal histidine) in MKT-IGC*c*P–CN$^-$ yields an NOE to an exchangeable signal at 10.1 ppm (signal f) (Figure 3b). The exchangeable nature of this proton was confirmed by performing the same experiment on a sample in D_2O, under which conditions no effect was observed at 10.1 ppm. The similar chemical shifts of signal f in HRP–CN$^-$ and MKT-IGC*c*P–CN$^-$ and the similar NOE extent for this signal in both proteins point to the assignment of signal f in MKT-IGC*c*P–CN$^-$ to Hδ1 of His-175. In addition, saturation of the β-CH (signal C) of this histidine in H_2O produces an NOE to signal f as well as to those previously reported[11e] on the other β-CH proton (signal F) and to the peptide amide proton (signal d) of the same histidine residue (Figure 3c). These connectivities are also detected in the NOESY map (Figure 5, cross peaks 25–29). If we compare the line width of signal f in the difference spectrum with that of a CH_3 signal that is at a known distance from the heme iron (i.e., 6.1 Å), we can see that the line width of both signals is similar. As typical histidine coordination to iron is associated with a shorter distance (5.1 Å), we conclude that the proximal histidine ligand to heme iron in MKT-IGC*c*P–CN$^-$ possesses significant imidazolate character as observed for HRP–CN$^-$. Identical NOE patterns are observed in C*c*P–CN$^-$. Collecting ^{1}H NMR spectra with fast repetition rates ($\leq$10 ms), we observed that a broad signal appears at 15.8 ppm in C*c*P–CN$^-$ and at 17.6 ppm in MKT-IGC*c*P–CN$^-$. Due to its fast relaxation rate and to its similarity with signal H′ in HRP–CN$^-$,[10c] we tentatively assign this signal as Hδ2 of the proximal histidine.

It is interesting to note that saturation of the resonance at −22.2 ppm yields an NOE also with a three-proton signal at −2.8 ppm. An NOE for this latter resonance is also observed by saturation of the 8-CH_3 resonance, exactly as found for HRP–CN$^-$. This signal can, therefore, be assigned to Leu-232, which is adjacent to both 8-CH_3 and Hϵ1 of His-175. Analogous 1D NOE results have been obtained for C*c*P–CN$^-$ (data not shown). Scalar connectivities observed in the COSY spectra (Figure 6, cross peaks 20, 21) on MKT-IGC*c*P–CN$^-$ allow us to assign the Hγ, δ-CH_3, and δ'-CH_3 signals of Leu-232. The NOESY map confirms the dipolar interaction of Leu-232 with 8-CH_3 (Figure 5, cross peaks 22–24). These observations provide further indication that both the coordination environments of the heme irons and the proximal environments of the heme groups of MKT-IGC*c*P–CN$^-$, C*c*P–CN$^-$, and HRP-CN$^-$ are highly similar.

The resonances of the distal histidine residue have been assigned previously for HRP–CN$^-$.[10d] While the signal at 14.0 ppm in C*c*P–CN$^-$ (signal G) has been proposed to arise from Hϵ1 of the distal histidine (His-52), no assignments have been reported for the exchangeable protons in the active site of C*c*P–CN$^-$. Saturation of signal G produces an NOE on two other resonances, signal a and signal c, for HRP–CN$^-$[10d] and MKT-IGC*c*P–CN$^-$ (Figure 4a and Figure 5, cross peak 30). In the latter case, we have verified that saturation of signal G in a sample in D_2O does not produce any NOE, thus confirming the nature of exchangeable protons of the signals that exhibit NOEs in water. From analogy with previous work with HRP–CN$^-$,[10d] these resonances are assigned as Hϵ2 and Hδ1 of His-52, respectively. Their different NOEs are consistent with their different T_1 values (see Table I). We conclude, therefore, that the distal histidine, His-52, is protonated in MKT-IGC*c*P–CN$^-$ as it is in HRP–CN$^-$.

The spectrum in H_2O of both C*c*P–CN$^-$ and MKT-IGC*c*P–CN$^-$ clearly shows two more hyperfine shifted exchangeable protons at 17.8 and 17.3 ppm (signal b) and at 12.3 and 12.2 ppm (signal e), respectively; only the latter is present in HRP–CN$^-$ at 12.9 ppm. In addition, from the analysis of the NOE data, it appears that for both C*c*P–CN$^-$ and MKT-IGC*c*P–CN$^-$, signal e is a composite signal with a broad shoulder (e′). In the case of C*c*P–CN$^-$, signal e′ displays an NOE upon saturation of signal G (Hϵ1 His-52) (Figure 4d). Upon saturation of signal b, an NOE is observed on signal G and on signal e′ (Figure 4e). The lack of the symmetrical NOE on signal b when saturating G could result from the short T_1 and large line width of the former signal. Saturation of the composite signal e gives only the reciprocal NOEs on G and b that, therefore, must originate from e′. Owing to the exchangeable nature of these protons, the observed NOEs could be simulated by actual saturation transfer effects. We have ruled out this possibility by performing the experiment at different temperatures (in the range 23–30 °C) and especially by collecting NOE difference spectra without excitation of the water protons (1331 pulse sequence[19]).

These NOE connectivities indicate that signals b and e′ belong to protons present in the distal cavity and close to Hϵ1 of the distal

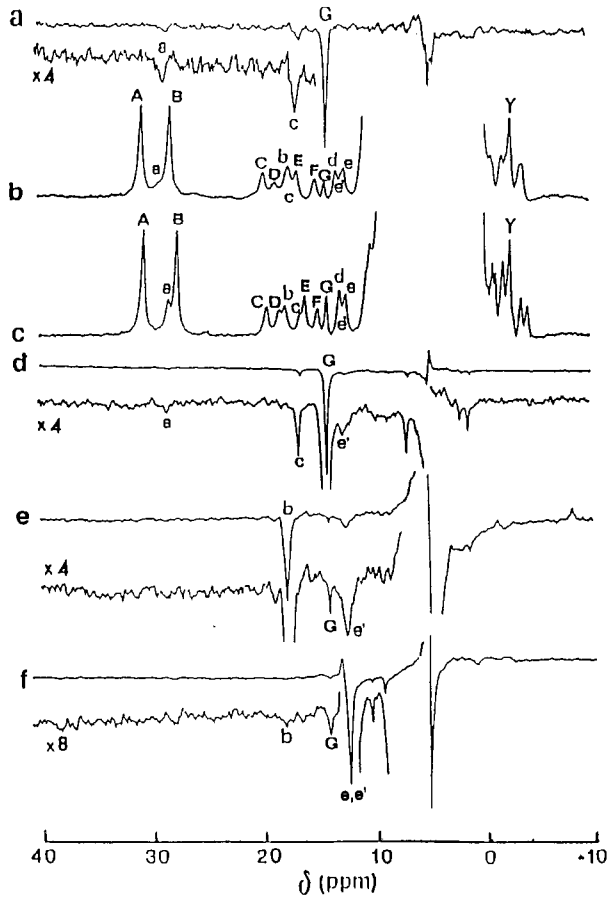

Figure 4. 200-MHz ^{1}H NMR spectra of water solutions of MKT-IGC*c*P–CN$^-$ (b) and C*c*P–CN$^-$ (c). Trace a is the NOE difference spectrum obtained upon saturation of signal G in MKT-IGC*c*P–CN$^-$. Traces d–f are the NOE difference spectra obtained upon saturation of signals G, b, and e,e', respectively, in C*c*P–CN$^-$. The experimental conditions are as in Figure 2.

His-52 residue. In the distal cavity, there are two more residues bearing exchangeable protons, Trp-51 and Arg-48. However, only the NHs of Arg-48 are close to Hε1 of the distal His and close to each other. At variance with the most recent NMR report,[12] we assign signal b to an exchangeable proton of Arg-48, as well as signal e'. Unfortunately, we cannot distinguish among the NH protons of this residue because quantitative estimates of interproton distances based on NOEs can be affected by exchange phenomena with bulk solvent. The exchangeable protons of Arg-48 are located above pyrrole IV and are expected to experience downfield pseudocontact shifts.[10b] In the case of MKT-IGC*c*P–CN$^-$, no NOEs between b and G and between e' and G are observed (data not shown), indicating that the position of Arg-48 is not the same in C*c*P–CN$^-$ and MKT-IGC*c*P–CN$^-$.

The COSY map of MKT-IGC*c*P–CN$^-$, collected in D_2O (Figure 6), clearly shows cross peaks between the previously assigned 4-Hβ_{cis} and 4-Hβ_{trans} (cross peak 1), 4-Hβ_{cis} and 4-Hα (cross peak 2), and 4-Hβ_{trans} and 4-Hα (cross peak 3). Another similar pattern of cross peaks is observed (cross peaks 4–6) that allowed us to assign 2-Hβ_{cis}, 2-Hβ_{trans}, and 2-Hα protons (see Table II). The NOESY connectivities confirm all of these assignments. NOESY cross peaks 7–9 identify the 7-Hα, 7-Hα', and 7-Hβ protons, in accord with previous results. The presence of both scalar and dipolar connectivities between the 7-Hβ proton and a signal at 3.0 ppm (cross peak 10) allows us to assign the latter as 7-Hβ'.

From Figure 2, it appears that subtle differences between the spectra of HRP–CN$^-$ and C*c*P–CN$^-$ may be meaningful. First, the positions of the 8-CH_3 and 3-CH_3 resonances in the two proteins are reversed as previously discussed in the literature.[11c] As the EPR spectra and presumably the magnetic anisotropies of HRP and C*c*P are similar,[20] the pseudocontact shift alone cannot account for the differences. This inversion is unusual in that the ordering of the 8-CH_3 to 3-CH_3 and 1-CH_3 to 5-CH_3 resonances is maintained in a large variety of heme-containing proteins,[26] even if the order of the two subsets of CH_3 signals (8/3 with 5/1) can be inverted as a result of a rotation of the axial ligand.[27,28] Another recently reported exception to the usual ordering of the 8-CH_3 to 3-CH_3 signals has been observed in the CN$^-$ adduct of lignin peroxidase (LiP).[29] This phenomenon has been explained previously on the basis of differences in peripheral heme–protein contacts.[11c] In particular, pyrrole II, which bears the 3-CH_3 group, is near Trp-51 in C*c*P, while the corresponding residue in HRP is a Phe (position 41). The 3-CH_3 experiences a greater isotropic shift in C*c*P–CN$^-$ than in HRP–CN$^-$ due to the greater charge-donating behavior of a Trp residue relative to a Phe residue. However, the same shift pattern is not experienced by the other protons of the vinyl group attached to the same pyrrole. On the other hand, this difference in shift pattern of 8-CH_3 and 3-CH_3 could also reflect some minor differences in the orientation of the proximal histidine residue in the two proteins. This hypothesis should be discussed in light of the signal positions of the latter group. The resonance of Hε1 of the proximal histidine is at −20.6 and −22.2 ppm in the case of C*c*P–CN$^-$ and MKT-IGC*c*P–CN$^-$, respectively, and at −29.9 ppm in the case of HRP–CN$^-$. The upfield shift of the imidazole Hε1 proton was proposed to be related to the imidazolate character of this ring on the basis of the shift values in model compounds.[30] The NH of that histidine (signal f), which is strongly hydrogen bonded to the carboxylate moiety of an Asp residue, shows approximately the same chemical shift for the three derivatives. This fact suggests that some geometrical arrangement of the proximal histidine, to which Hε1 is highly sensitive, is operative, possibly depending on the imidazolate character of this residue. Consistent with this, the shift separation between the signals of the β-CH_2 of the same residue is significantly different (8.1 ppm in HRP–CN$^-$ and 4.6 ppm in C*c*P–CN$^-$). The contact shifts of the β-CH_2 protons depend on the dihedral angle between the imidazole plane and the C_γ–C_β–H plane. The larger separation of these shifts and the larger differences in T_1 values seen in HRP–CN$^-$ are indicative of an axial and equatorial nature of the β-CH_2 protons with respect to the imidazole plane. From the line shape and T_1 values, it appears that the two protons have similar distances from the metal ion in the case of C*c*P–CN$^-$, which is consistent with the smaller shift separation.

It appears that the three signals (a, c, G) assigned to protons of the distal histidine residues experience essentially identical hyperfine shifts in the three derivatives. The distal histidine residue is never bound to the iron, and the proton shifts are expected to be largely pseudocontact in origin.[31] As pseudocontact shifts depend on the magnetic susceptibility tensor, it may be concluded that the latter is the same in the three systems. The peptide NH proton of the proximal histidine experiences some hyperfine shift, as indicated by the temperature dependence of its chemical shift. As this proton is separated from the metal ion by several bonds, its hyperfine shift is essentially pseudocontact in origin. From a comparison of the chemical shift values for this signal (d) in C*c*P–CN$^-$ and HRP–CN$^-$ (Table I), it appears that these resonances are identical, thus further indicating that the magnetic susceptibility tensor is the same in the two systems. This confirms that the isotropic shift differences of protons of the bound groups

(26) (a) Blumberg, W. E.; Peisach, J.; Wittenberg, B. A.; Wittenberg, J. B. *J. Biol. Chem.* **1968**, *243*, 1854. (b) Wittenberg, B. A.; Kampa, L.; Wittenberg, J. G.; Blumberg, W. F.; Peisach, J. *J. Biol. Chem.* **1968**, *243*, 1863.
(27) Keller, R. M.; Wüthrich, K. *Biochem. Biophys. Res. Commun.* **1978**, *83*, 1132.
(28) Keller, R. M.; Schejter, A.; Wüthrich, K. *Biochem. Biophys. Acta* **1980**, *626*, 15.
(29) Banci, L.; Bertini, L.; Turano, P.; Tien, M.; Kirk, T. K. *Proc. Natl. Acad. Sci. U.S.A.* **1991**, *88*, 6956.
(30) Chacko, V. P.; La Mar, G. N. *J. Am. Chem. Soc.* **1982**, *104*, 7002.
(31) Emerson and La Mar (*Biochemistry* **1990**, *29*, 1545) have suggested that the shift of Hε2 in cyanometmyoglobin experiences some contact contributions. This is still consistent with the present conclusions.

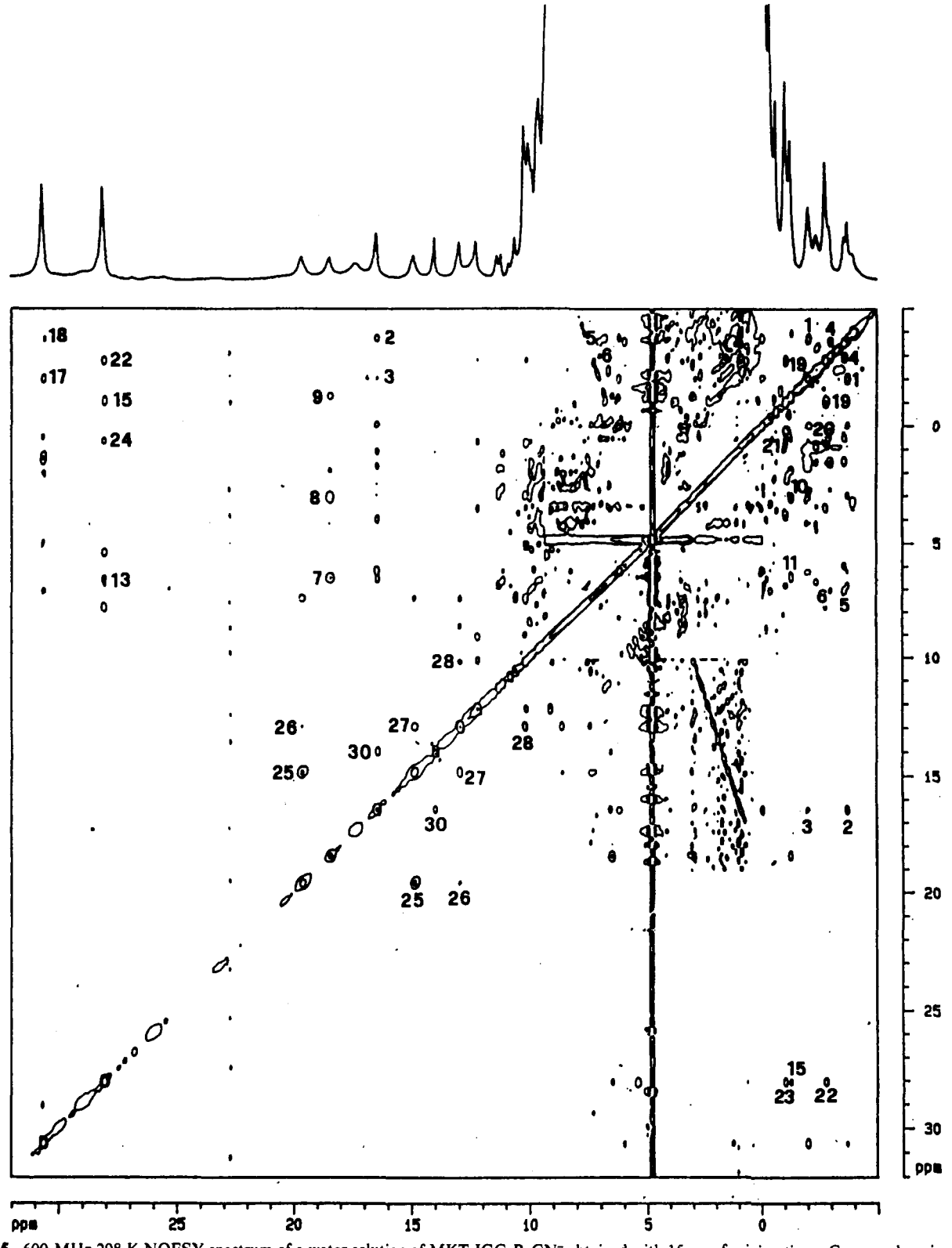

Figure 5. 600-MHz 298 K NOESY spectrum of a water solution of MKT-IGCcP–CN^- obtained with 15 ms of mixing time. Cross peak assignments: (1) 4-Hβ_{cis}, 4-Hβt_{rans}; (2) 4-Hα, 4-Hβ_{cis}; (3) 4-Hα, 4-Hβ_{trans}; (4) 2-Hβ_{cis}, 2-Hβ_{trans}; (5) 2-Hα, 2-Hβ_{cis}; (6) 2-Hα, 2-Hβ_{trans}; (7) 7-Hα, 7-Hα'; (8) 7-Hα, 7-Hβ'; (9) 7-Hα, 7-Hβ; (10) 7-Hβ, 7-Hβ'; (11) 7-Hα', 7-Hβ; (12) 8-CH_3, 7-Hα; (13) 8-CH_3, 7-Hα'; (14) 8-CH_3, 7-Hβ'; (15) 8-CH_3, 7-Hβ; (16) 3-CH_3, 4-Hα; (17) 3-CH_3, 4-Hβ_{trans}; (18) 3-CH_3, 4-Hβ_{cis}; (19) δ'-CH_3 Leu-232, δ-CH_3Leu-232; (20) Hγ Leu-232, δ-CH_3 Leu-232; (21) Hγ Leu-232, δ'-CH_3 Leu-232; (22) 8-CH_3, δ-CH_3 Leu-232; (23) 8-CH_3, δ'-CH_3 Leu-232; (24) 8-CH_3, Hγ Leu-232; (25) Hβ His-175, Hβ' His-175; (26) Hβ His-175, NH_p His-175; (27) Hβ' His-175, NH_p His-175; (28) Hβ' His-175, Hδ1 His-175; (29) Hβ His-175, Hδ1 His-175; (30) Hδ1 His-52, Hϵ1 His-52. Cross peaks 12, 14, 16, and 29 become observable by decreasing the threshold.

are due to subtle structural changes. On the other hand, the NOEs between Hϵ1 of the proximal histidine and the δ-CH_3 of the nearby Leu residue (Leu-232 in CcP and Leu-237 in HRP) are the same within experimental error. This fact suggests no major structural variations on the residues of the proximal side.

In summary, the substantial similarity of the magnetic anisotropy tensors for CcP–CN^- and HRP–CN^- demonstrates that the electronic structures of the active sites of the two proteins are very similar. The distal imidazole is protonated at neutral pH in the cyanide complexes of both proteins, while the chemical shifts of the proximal histidine protons indicate some minor rearrangements of this residue. Such rearrangements affect the Hϵ1

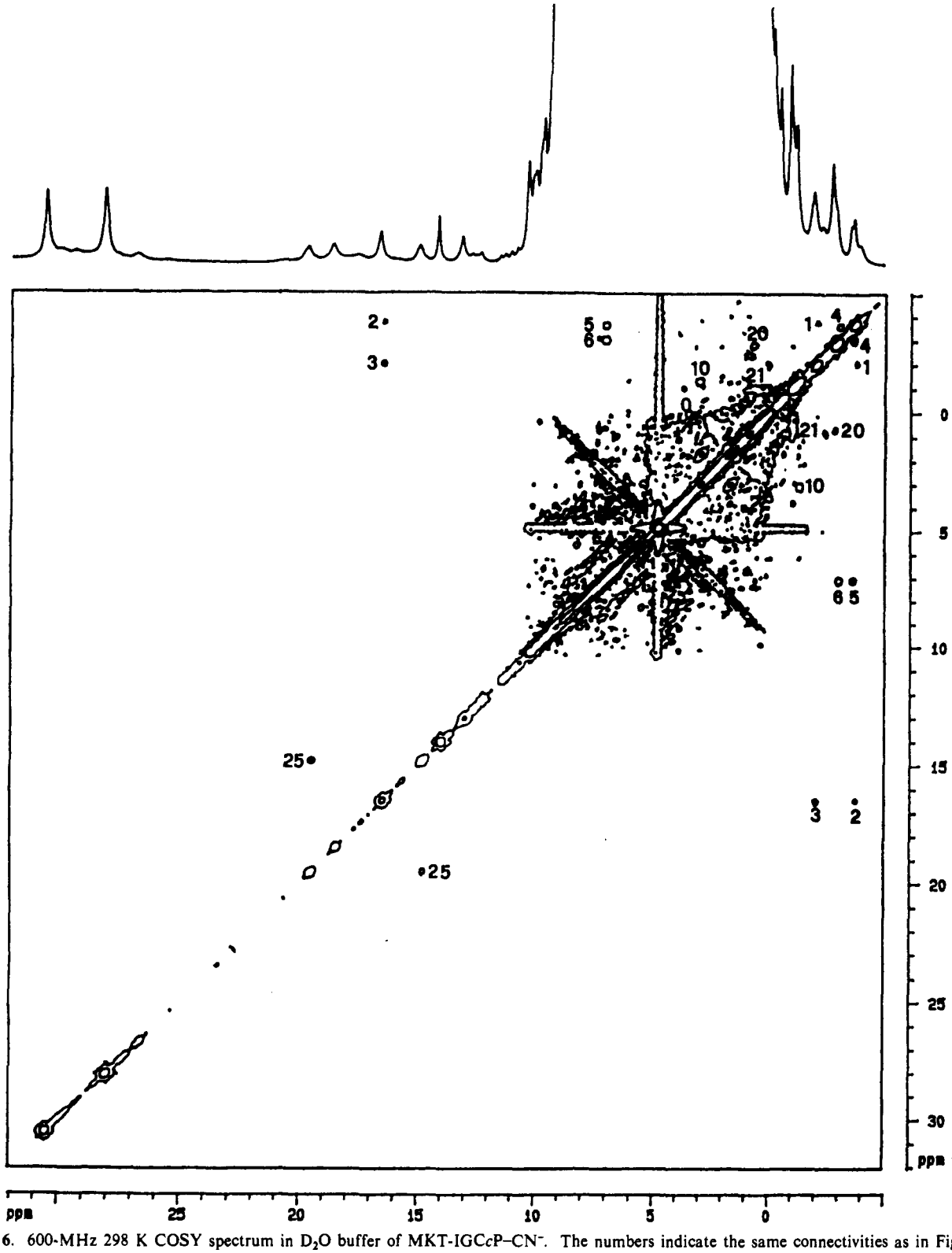

Figure 6. 600-MHz 298 K COSY spectrum in D_2O buffer of MKT-IGC*c*P–CN^-. The numbers indicate the same connectivities as in Figure 5.

and the β-CH_2 protons but not Hδ1 or peptide NH. An even smaller upfield shift for the Hϵ1 and a smaller separation in shift for the β-CH_2 protons of the proximal histidine has been observed for the CN^- adduct of LiP.[29] The pattern of the shifts for these signals with the reduction potential of the protein has been shown to correlate.[29] A more extensive pattern of exchangeable proton signals is observed in C*c*P–CN^- and MKT-IGC*c*P–CN^- than for HRP–CN^-. The difference in interproton connectivities (and, therefore, in distance between Arg-48 and Hϵ1 of His-52) observed for C*c*P–CN^- and MKT-IGC*c*P–CN^- may result from the presence of an Thr residue at position 53 in the former protein and a Ile residue at this position in the latter protein. In addition, the line width of the proton bridging His-52 and CN^- is sensitive to the conditions of sample preparation and in particular to the age of the sample.

Acknowledgment. This work was supported by Grant MT-7182 from the Medical Research Council of Canada (to A.G.M.), and a postdoctoral fellowship from the Ministerio de Educación y Ciencia of Spain (to J.C.F.). We thank Dr. David B. Goodin for the recombinant MKT-IGC*c*P expression system, Professor Brian Hoffman and Eric Stemp for a sample of cytochrome *c* peroxidase isolated from baker's yeast, and Professor Thomas Poulos for the coordinates of the C*c*P–CN^- complex.